A Study of Cu(I)-Ethylene Complexation for Olefin–Paraffin Separation

Joseph Chen and R. Bruce Eldridge
Process Science and Technology Center, Cockrell School of Engineering, The University of Texas, Austin, TX 78712

Evelyn L. Rosen and Christopher W. Bielawski
Dept. of Chemistry and Biochemistry, The University of Texas, Austin, TX 78712

DOI 10.1002/aic.12286
Published online July 13, 2010 in Wiley Online Library (wileyonlinelibrary.com).

The current cryogenic distillation technology used for olefin–paraffin separation incurs extensive capital and operating costs. An alternative olefin–paraffin separation process, based on reactive absorption, could yield significant cost reductions. The research efforts described herein explored the structural characteristics of an NMP-CuCl-aniline absorption solution with ethylene to aid future development of olefin–paraffin separation systems. Solution IR and ^{1}H NMR spectroscopy suggested weak and labile Cu(I)-ethylene and Cu(I)-aniline coordination, which point to the coexistence of multiple structures in solution. Experiments also revealed solvent-dependent and temperature-dependent coordination. The agreement of the collected spectral data with literature implied single ethylene coordination, whereas the Cl^- ion likely remained coordinated with Cu(I). Solvent interference prohibited detailed investigation of IR spectra, but ^{1}H NMR spectroscopy showed more promise as an analytical technique for the NMP-CuCl-aniline-ethylene system. Finally, a tradeoff appears to exist between ethylene capacity and complex stability, and thus, an optimal ligand must be found that balances these two competing needs. © 2010 American Institute of Chemical Engineers
AIChE J, 57: 630–644, 2011
Keywords: olefin-paraffin separation, reactive absorption, π-bond complexation

Introduction

The separation of olefins from paraffins serves as a key process in the production of many industrial chemicals such as ethylene (95 million tons produced in 2002) (Reine, Unpublished doctoral dissertation). This separation currently utilizes cryogenic distillation, an energy-intensive and expensive process. Because of the similar boiling points of olefins and paraffins (184.6 K for ethane and 169.4 K for ethylene)[1] large distillation columns with up to 150 trays and diameters exceeding 5 m must be operated at temperatures as low as −90°C and pressures as high as 20 atmospheres. This technique uses exorbitant amounts of energy. Cryogenic distillation alone consumes 0.1 quads of energy annually, accounting for 6.2% of the total energy used in all distillation processes. An alternative olefin–paraffin separation process with lower energy consumption would significantly decrease operating expenses. Furthermore, a less-expensive process could improve the economic viability of separating smaller olefin–paraffin sources. Because of the enormous cost of cryogenic distillation, these sources are currently burned as fuel, wasting the superior chemical characteristics of the olefins and discarding otherwise valuable product.

Reactive absorption with Cu(I)-based solutions can serve as an energy-efficient alternative to cryogenic distillation. The Cu(I) ion possesses a unique orbital structure that allows for complexation with a carbon–carbon double bond.[2] As paraffins do not contain double bonds, a copper absorption

Correspondence concerning this article should be addressed to R. B. Eldridge at rbeldr@che.utexas.edu.

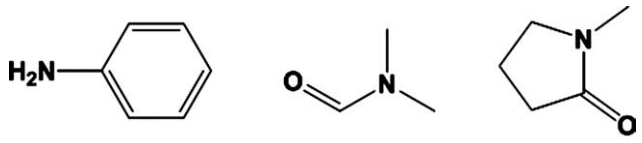

aniline DMF NMP

Figure 1. Structures of aniline, dimethylformamide (DMF) and *N*-methylpyrrolidine (NMP).

system that can separate an olefin–paraffin mixture on the basis of these electronic differences should be possible. Such an absorption method eliminates the need for refrigeration, thus increasing energy efficiency and reducing capital cost.

Reine and Eldridge explored the capacity for ethylene absorption of various Cu(I) solutions with a focus on using low cost, industrially feasible materials.[1,3,4] A combination of CuCl, aniline, and *N*-methylpyrrolidone (NMP) exhibited optimal solution characteristics, including low cost, high ethylene capacity, low volatility, and high stability. However a lack of basic understanding regarding the structure of the Cu(I)-ethylene-aniline complex impedes the development of reactive absorption systems. Therefore, this study focused on elucidating structural information, including the Cu(I)-ethylene and Cu(I)-aniline complexation, by analyzing the solution using IR and ^{1}H NMR spectroscopy. X-ray crystallography was also explored as a possible characterization technique. Developing such structural knowledge was expected to yield the number of ethylene molecules bound per molecule of copper, information that can be used to estimate the maximum ethylene capacity for a given solution. Furthermore, this study hopes to clarify how various types of ligands can coordinate with Cu(I) and protect the metal ion from deactivation. In actual operation, feed streams can contain trace impurities such as oxygen or H_2S, which will degrade and eventually deactivate the solution by oxidizing Cu(I) to Cu(II). Thus, information on metal–ligand coordination can aid in the design of degradation-resistant absorption solutions.

Background and Theory

Previous work on CuCl-aniline-NMP system

Reine and Eldridge conducted extensive research on the Cu(I)-ethylene system for reactive absorption.[4] The capability for a solution of CuCl or CuBr in dimethylformamide (DMF) to chemically absorb ethylene was proven via cyclic voltammetry (CV). Various ligands, such as aniline, benzylamine, and pyridine, were added to the system during the tests to aid solvation of CuCl and protect the copper ion from contaminants. CV experiments proved that the combination of the weaker anion Cl^- and the weakest ligand aniline yielded the highest capacity for ethylene, as they would be more easily displaced by ethylene molecules.[4] However, due to health concerns over the use of DMF as solvent, DMF was replaced with *N*-methylpyrrolidone (NMP), a chemically similar solvent. For reference, Figure 1 below shows the structures of aniline, DMF, and NMP. Reine also performed kinetic studies on the CuCl, aniline, and DMF system.[3] These experiments indicated a 1:1 Cu(I) to ethylene ratio in the metal–olefin complexes and a first-order reaction, as shown in Eq. 1.

$$C_2H_4 + Cu^+ \rightleftharpoons Cu^+C_2H_4 \quad (1)$$

Even though the reaction data fit the first-order reaction model, the calculated ethylene concentration in the solution was only half that of the copper solution. It was concluded that the ligand was most likely coordinating with Cu(I) ion, blocking approximately half the sites from ethylene.

Metal-olefin complexation

The novel reactive absorption system described above utilizes metal–olefin complexation as a basis for separation. The well-established fundamentals of metal–olefin interactions begin with the classic Dewar-Chatt-Duncanson model.[1,5] In general, this model states that the π-bond in ethylene can donate into a vacant orbital on the metal atom to which it is ligated, allowing for the formation of a σ-bond. Furthermore, filled metal *d*-orbitals with the proper symmetry can overlap with the empty ethylene π^*-antibonding orbitals, forming two π-bonds in a process that is called π-backbonding. Figure 2 illustrates these interactions.[2]

This backbonding in metal–olefin complexes contributes to the stability of the complex by allowing the electron-rich metal center to dissipate excess electron density through donation to the ligated ethylene unit. The importance of π-backbonding vs. σ-bonding interactions in metal–olefin complexes varies with the metal and coordinated ligands. Normally, the σ component dominates whereas the π component adds a small but significant contribution to the overall strength of the metal–olefin bond.[6–10] The π backbonding interaction affects the carbon–carbon bond in ethylene; due

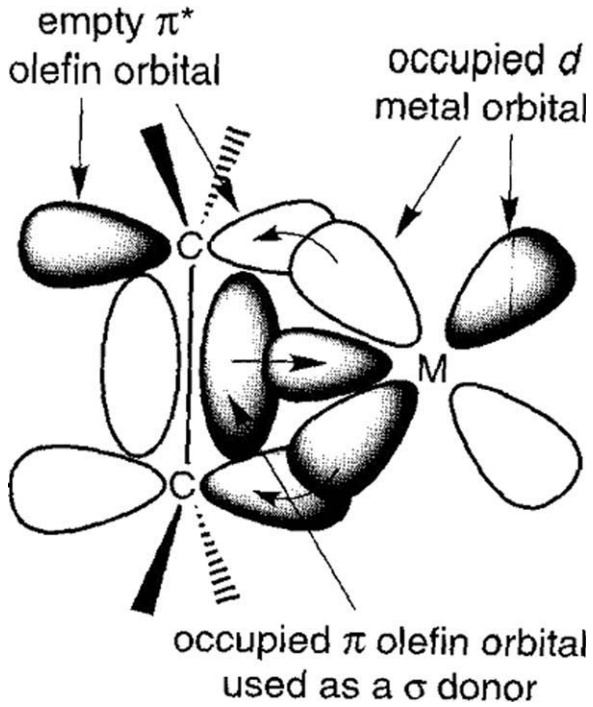

Figure 2. Complexation of metal and ethylene.

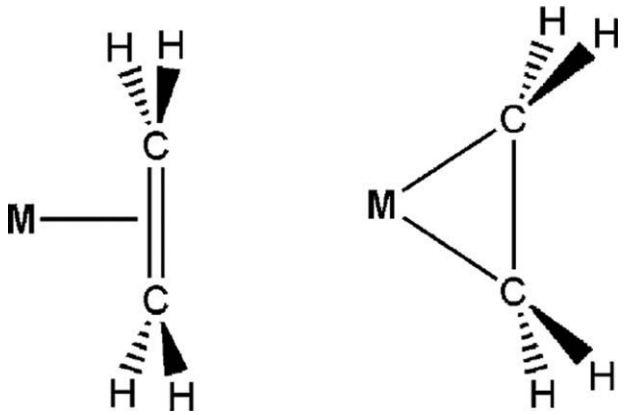

Figure 3. Extremes of σ and π bonding (left and right, respectively).

to population of the π^* antibonding orbital, the π character of the double bond is reduced. Thus, the carbon–carbon bond length increases, indicating a weakening of the bond.[2,11] As expected, the carbon–carbon bond length approaches that of a single bond as π backbonding increases. Figure 3 below illustrates the two extremes of σ-bonding (left) and π-bonding (right) interactions.[7]

The effect of metal complexation on ethylene bond length can be observed directly through X-ray crystallography and indirectly through changes in vibrational and NMR spectra of the respective complexes. Relevant spectroscopic analyses will be discussed in greater detail below.

Notably, other metals in the same family, such as silver and gold, form comparable complexes with ethylene, as they have similar valence characteristics as copper. Experimental results and theoretical calculations reveal that bonding strength increases in the order of Ag(I) < Cu(I) < Au(I).[7,12–15] Gold is better than copper in bond strength, but due to the high cost of gold (and silver), copper remains the most economical choice for a reactive absorption system.

Ligand complexation

The Cu(I)-ethylene complex alone is unstable and labile, and thus, additional ligands are used to increase stability. Furthermore, additional ligands can protect and stabilize the naturally unstable Cu(I) ion from disproportionation,[5] increase ethylene capacity by sterically preventing the olefin from dissociating, and separate α-olefins (terminal olefins) from branched or internal olefins through steric hindrance.[16] The current study will focus on exploring various ligands and their roles in influencing Cu(I)-ethylene complexes. In particular, these effects will be discussed in conjunction with a variety of spectroscopic and other experimental measurements.

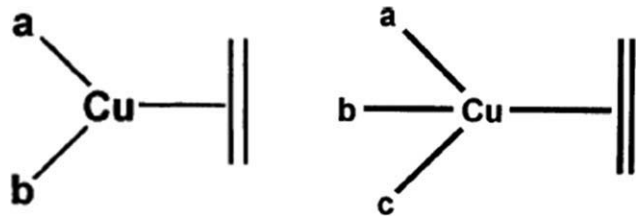

Figure 4. Common Cu(I)-ethylene structures.

Ligands can be monodentate or polydentate. Monodentate ligands bind to the metal through one donor atom, whereas polydentate ligands donate through two or more atoms. In general, polydentate ligands stabilize the copper complex to a much greater degree than monodentate ligands due to entropic effects.[17] Notably, aniline acts as a monodentate ligand which, in light of the previous discussion, implies a relatively weak ability to complex to various metals, including Cu. Literature points strongly toward the interaction between the amino group of aniline and Cu(I) being most dominant,[10,11,18] though a study by Ruan et al. calculated that the most stable Cu(I)-aniline interaction involved the Cu(I) ion associating with a single double bond in aniline's aromatic ring.[9]

In nearly all of the reported structurally characterized Cu(I)-ethylene compounds, the auxiliary ligand acts as a bidentate or tridentate ligand. Given a bidentate ligand, the complex forms a trigonal planar structure.[8,10,11,13,19–23] Given a tridentate ligand, the complex forms a distorted tetrahedral structure.[22,24,25] Figure 4 below illustrates these two structures, where a, b, and c represent ligand attachment sites.[23]

Although this seems straightforward, the coordination number of the ligand can vary significantly with minor chemical changes. Thompson et al. found that methylation of the ligand hydrotris(1-pyrazolyl) borate, or $HBpz_3$, to hydrotris(3,5-dimethyl-l-pyrazolyl) borate, or $HB(3,5\text{-}Me_2pz)_3$, can change the coordination from trigonal planar to distorted tetrahedral, respectively. Figure 5 below illustrates

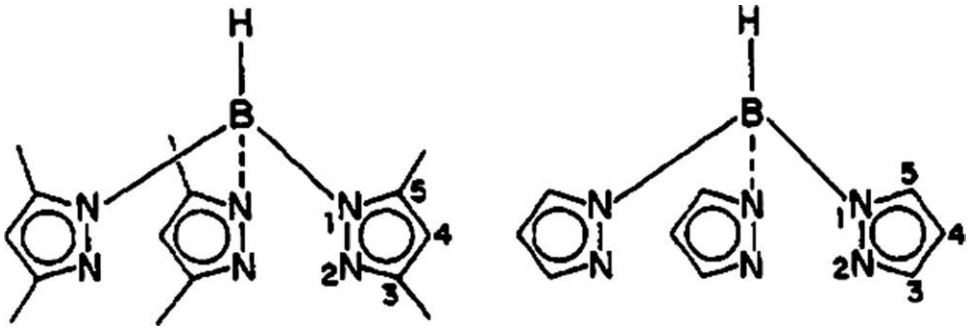

Figure 5. $HB(3,5,\text{-}Me2pz)_3$ left and $HBpz_3$ right.

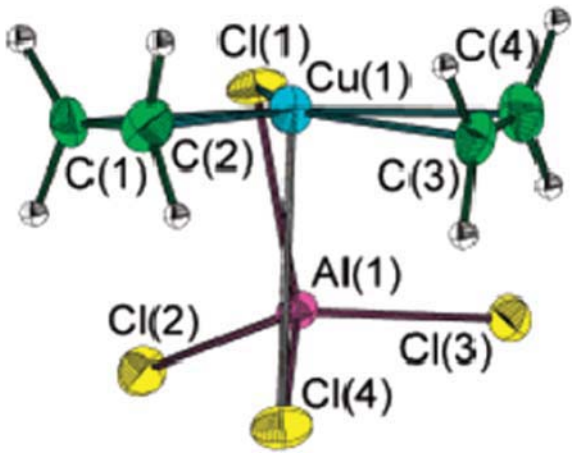

Figure 6. Cu(I) ion with two ethylene molecules in a unique structure.

[Color figure can be viewed in the online issue, which is available at wileyonlinelibrary.com.]

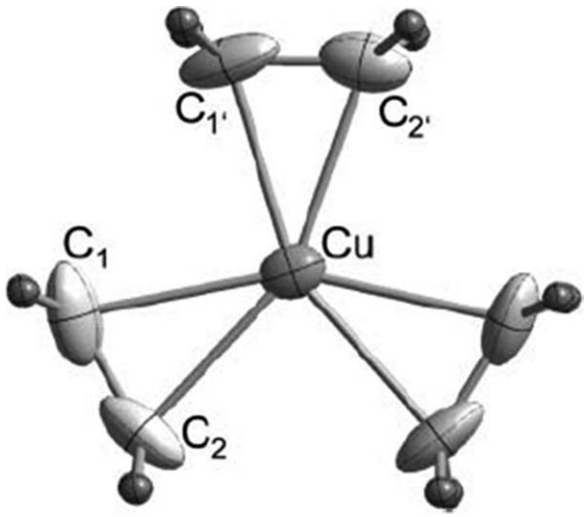

Figure 7. Three ethylene adducts on Cu(I).

the two ligands, which are nearly the same except for two methyl groups on each pyrazolyl group.[22]

Furthermore, there exists several rare exceptions where multiple ethylene units can fill coordination sites on the Cu(I) ion. Sullivan et al. formed $(C_2H_4)CuAlCl_4$ and $(C_2H_4)_2CuAlCl_4$ complexes by adsorbing ethylene gas onto crystals of $CuAlCl_4$. The former possesses a tetrahedral structure as shown above. The latter has a coordination number of four, but forms a trigonal-planar arrangement with two ethylenes and one Cl atom. The last coordination site is filled with another Cl atom from an $AlCl_4$ group. This "plane + 1" structure is shown below in Figure 6.[25]

Copper compounds with three ethylene adducts have also been synthesized through the use of weak coordinating anions.[12,26] Both form a trigonal planar structure, as shown below in Figure 7.

If the olefin bound in the complex is not ethylene, many other types of structures are possible. For example, olefins with multiple double bonds may act as polydentate ligands. Munakata et al. synthesized $[Cu(1,5\text{-cyclooctadiene})_2]ClO_4$ in which four alkene groups ligate the copper atom.[27] Figure 8 below shows the X-ray crystal structure as well as a bonding schematic.[23,27]

Large molecules with only one double bond can interact with the copper through other atoms. Zaklika et al. synthesized [Cu(diethylentriamine)norbornene]$^+I^-$ and found that a hydrogen atom from norbornene interacted with the Cu(I) center due to its proximity to the ion.[18] In summary, despite the general consensus on trigonal planar or distorted tetrahedral structures for Cu(I)-ethylene complexes, the choice of ligand and the variation of the olefin can significantly affect the coordination structure.

Unfortunately, virtually no literature addresses the structure of CuCl-ethylene complexes with aniline as a supporting ligand, most likely because of complex lability and instability. However, from the literature discussed above, the structure of a CuCl-ethylene-aniline complex should be either trigonal planar or tetrahedral if the coordination sites on Cu(I) are all filled. The nitrogen atom in NMP would be unlikely to bind due to the conjugation of the lone pair of electrons on the nitrogen atom with the carbonyl. In contrast, Cl^- most likely remains coordinated with the Cu(I) ion, donating charge through one of its lone pairs.[23,26] The Cl^- ion can also bridge multiple Cu(I) ions, although this is generally not seen with aniline or ethylene as ligands.[23,28] Thus, the ethylene and Cl^- would each occupy one coordination site, whereas aniline would most likely fill the others. Because of the weak coordination of aniline to copper, Cu(I) ions with one or more empty coordination sites would probably exist in equilibrium with the fully coordinated species.

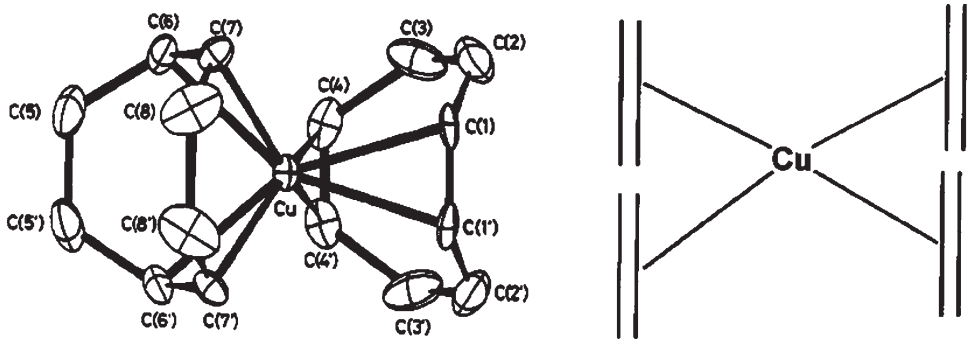

Figure 8. $[Cu(1,5\ cyclooctadiene)_2]ClO_4$ and bonding schematic.

Effects of complexation and spectroscopic analysis

As mentioned before, the ethylene double bond decreases in bond order during complexation with the Cu(I) ion. This study proposes to use infrared (IR) spectroscopy and proton nuclear magnetic resonance (^{1}H NMR) spectroscopy as the primary methods to investigate the effects of complexation on ethylene, and thus, these two techniques will be discussed in detail. However, X-ray crystallography data on various complexes will also be discussed. Finally, the effects of complexation on the ^{1}H NMR and IR spectra on auxiliary ligands such as aniline will be described in detail.

IR spectroscopy reveals that the vibrational frequency of the olefin C=C bond, which normally manifests itself as a weak signal at ~1623 cm^{-1}, shifts to lower frequencies upon complexation due to the reduction in the bond force constant. In general, the greater the shift, the greater the decrease in π-character of the bond, and thus the formation of a stronger olefin–metal interaction.[8,11] However, this shift can vary significantly depending on the type of auxiliary ligand used. Sunderrajan et al. formed a complex with $AgBF_4$ and $AgCF_3SO_3$ with 1-hexene in chloroform and observed a shift from 1640 cm^{-1} (uncomplexed) to 1585 cm^{-1}.[29] Suenaga et al. used tetramethylethylenediamine (tmen) to form a $[Cu(tmen)C_2H_4]^+ClO_4$ complex. The ethylene vibration shifted to 1525 cm^{-1}, a shift of 98 cm^{-1} from uncomplexed ethylene (1623 cm^{-1}).[11] Other studies found shifts to 1550 cm^{-1} and 1577 cm^{-1} for Cu(I)-ethylene compounds.[24,26] Although the reason for these differences are not well explained in literature, the IR shift serves as a useful identification for Cu(I)-ethylene coordination.

^{1}H NMR spectroscopy shows that the ethylene peak, normally found at $\delta \sim 5.24$ ppm, usually shifts upfield upon complexation. As complexation draws away some of electron density, the anisotropic effect present in ethylene is decreased, and thus, an upfield shift is observed.[30] The amount of shift varies depending on the auxiliary ligands. Santiso-Quinones et al. and Dias et al. synthesized $[Cu(C_2H_4)_3]^-$ with different counter ions, and both displayed a slight *downfield* shift from $\delta = 5.24$ ppm to $\delta = 5.44$–5.47 ppm.[12,26] On the other hand, Dai and Warren formed a complex of CuBr-SMe_2 with thallium β-diketiminate and ethylene, and the ethylene peak was observed far upfield at $\delta = 2.91$ ppm.[19] Most Cu(I)-ethylene complexes span these two extremes of ^{1}H NMR chemical shifts.[8,10,11,13,20,22,24] The amount of the chemical shift has been hypothesized to increase with increasing basicity (pKa) of the auxiliary ligands, as increasingly basic ligands will donate more electron density to the Cu(I) ion. The metal center sheds this electron density through increased π-backbonding, which will increase the chemical shift of the signal observed.[7,8,11,20] Figure 9 below illustrates this effect for an array of ligands of Cu(I)-ethylene complexes.[8]

The ethylene ^{1}H NMR signal appears as a single peak, indicating the fast exchange of uncomplexed and complexed ethylene. Addition of excess ethylene broadens this peak, which supports the existence of a labile interaction.[13]

Another common method used to investigate Cu(I)-ethylene complexation is X-ray crystallography. X-ray crystallography should show that complexation increases the alkene bond distance, and indeed, this is often the case.[10,11,19,20,22] However, this bond lengthening is far less than that predicted given the degree of change in the vibrational spectra.[10,22] In fact, in the tris-ethylene complex $[Cu(C_2H_4)_3]^-$, no significant bond lengthening is observed,[12,26] and most increases in bond length are on the order of magnitude of the errors inherent to X-ray crystallography. This contradiction has been explained by applying the concept of Rydberg orbitals.[7,23] Also, olefins located in rings tend to lengthen more due to the relief of ring strain.[21]

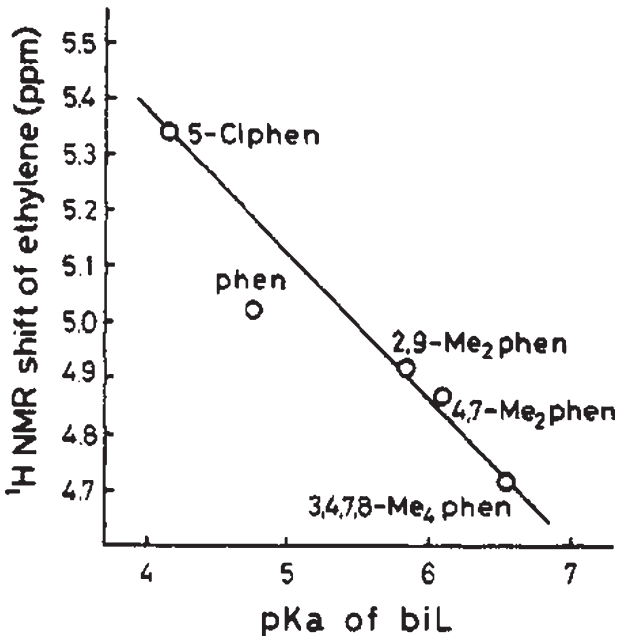

Figure 9. Effect of ligand basicity on 1H NMR shift for phenanthroline and its derivatives.

Complexation with copper also affects auxiliary ligands, again, by drawing away electron density. In general, this reduces the force constants of the bonds around the coordinated atom. A number of sources used infrared spectroscopy to explore the effects of complexation on aniline. Some focused on studying the Cu(I)-aniline bond, where coordination through the nitrogen atom causes the N—H stretching and bending frequencies to decrease. However, the effect of complexation on the aromatic ring remains unsettled.[31,32] A greater number of sources explored the Cu(II)-aniline bond due to the greater stability of Cu(II) compared with Cu(I). Complexation of Cu(II)-aniline exhibits similar characteristics as Cu(I)-aniline, showing a decrease in N—H stretching (100–200 cm^{-1}) and bending frequencies (15–50 cm^{-1}).[33–36] The amount of change in frequency varied directly with the basicity of the ligand,[34] and little effect on the aromatic ring was observed.[36] Akalin and Akyuz cited an increase in the N—H twisting and wagging frequencies which was explained by hybridization changes causing variations in molecule geometry.[33] Akyuz and Davies noted a decreasing N—H frequency with decreasing temperature, indicating a stronger interaction with lower temperatures.[37] Finally, infrared spectroscopy was used to verify the presence of a metal-nitrogen and metal-halide bonds in various metal(II) halide-aniline complexes. For $CuCl_2$, the metal-nitrogen bond displayed two peaks at 434 and 359 cm^{-1}, whereas the metal-halide bond appeared at 298 and 273 cm^{-1}.[36] Thus, infrared

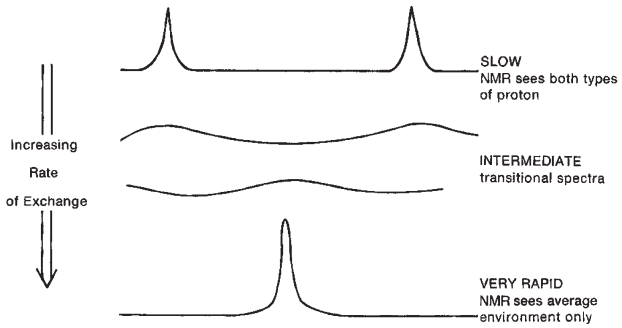

Figure 10. Peak broadening due to chemical exchange.

spectroscopy can verify coordination bonds as well as investigate the effects of coordination on auxiliary ligands.

The effects of complexation on ligands can also be explored using ^{1}H NMR spectroscopy. In general, this can be seen through a downfield shift in ^{1}H NMR signal, as reducing electron density decreases shielding.[8,11,34,38,39] Furthermore, reversible coordination events which are faster than the NMR timescale can broaden the observed signals attributed to the ligand.[40–42] Figure 10 below illustrates peak broadening, or line broadening, for two magnetic states.[30] Given a slow exchange rate, peaks representing each magnetic state are resolved separately. As the exchange rate increases, the peaks begin to coalesce and a broad resonance peak spanning the separation in shift is seen. At fast exchange rates, the ligand experiences all magnetic states at once, which results in a single peak representing the average magnetic state.[40,43] Monodentate aniline can yield a large variety of labile complexes with varying stoichiometries, which promotes line broadening.[42] Finally, the presence of a quadrupole moment in the nitrogen nuclei of aniline can be another source of peak broadening, though this effect depends on solvent environment and temperature.[30] Thus, peak broadening will probably occur with Cu(I)-aniline complexation, though the degree of broadening will depend on the exchange rate, complex formations, and environmental conditions.

Experimental Procedures and Apparati

Preliminary experiments

Given the unambiguous structural characterization afforded by X-ray crystallography, preliminary experiments aimed to crystallize a relevant complex. An apparatus was constructed to deliver ethylene to the CuCl-aniline-NMP mixture at low temperatures (−15°C) with limited air and moisture exposure. Figure 11 below illustrates the experimental apparatus used in the preliminary experiments.

CuCl, NMP, and aniline were added to the reaction flask under a flow of nitrogen. After connecting the reaction flask to the apparatus, ethylene was sparged through the solution to form the complex. Then, the reaction flask was isolated

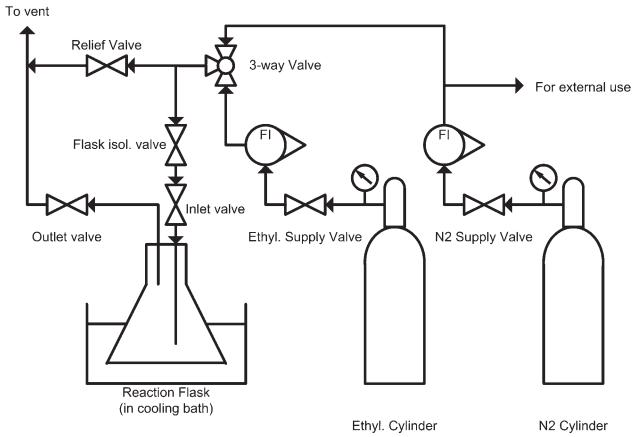

Figure 11. PFD of apparatus.

and chilled down from room temperature to −15°C for 6 h. Finally, the solution in the flask was inspected for formation of crystals as well as other qualitative observations.

IR experiments

To investigate the Cu(I)-ethylene and Cu(I)-aniline interaction in NMP, the following solutions were prepared for IR spectroscopic analysis: NMP and aniline (IR Solution 1); NMP, aniline, and CuCl (IR Solution 2); and NMP, aniline, CuCl, and ethylene (IR Solution 3). To prevent air and moisture contamination, the aniline and NMP were both dried and degassed by three consecutive freeze-pump-thaw cycles. Also, all solutions were prepared in a nitrogen filled dry box. Table 1 below details the amounts of reagents used for IR Solution 2 and IR Solution 3.

The amounts of reagents used in IR Solution 1 were not recorded, as the solution contained only NMP and aniline to serve as a baseline. Also, the aniline:CuCl ratio was decreased from IR Solution 2 to Solution 3 to promote ethylene complexation by decreasing the number of coordination sites occupied by aniline. To prepare the solution with ethylene, the NMP-aniline-CuCl solution was transferred to a Schlenk flask, and the solution was stirred under a >50 ml/min flow of ethylene for 5 min. The flask was then stirred under an atmosphere of ethylene for 2 h.

Additional IR tests were conducted using methanol as a solvent, as methanol contains fewer functional groups than NMP. Thus, infrared spectra taken in methanol should exhibit less solvent interference. Table 2 below shows the reagents used for the solutions made for these tests.

Because of difficulties in adding ethylene to the solution, this step was omitted with methanol. The methanol tests were conducted on the benchtop and not in the dry box. Thus, air and moisture contamination occurred, and the effects of contamination were considered during analysis.

Table 1. IR Solutions with NMP

Name	NMP	Aniline	CuCl	Ethylene (138 kPa)	CuCl Concentration	Aniline:CuCl Molar Ratio
IR solution 2	1.2 mL	0.08 mL	25 mg	No	0.26 M	1.99:1
IR solution 3	8.5 mL	0.4 mL	222.8 mg	Yes	0.21 M	3.55:1

Table 2. IR Solutions with MeOH

Name	MeOH	Aniline	CuCl	Ethylene (138 kPa)	CuCl Concentration	Aniline:CuCl Molar Ratio
IR solution 4	1 mL	0.05 mL	–	No	–	–
IR solution 5	1 mL	0.02 mL	20 mg	Yes	0.198 M	1.1:1

A Perkin-Elmer Spectrum BX FTIR spectrometer was used in conjunction with a CaF_2 sealed liquid cell to acquire the IR spectra of the aforementioned mixtures. The IR cell was loaded with the solution in the dry box, and then transferred to the spectrometer for analysis. Notably, the IR cell was not airtight, though plugs on the solution injection ports provided a measure of protection, as did the short transfer times from dry box to spectrometer. Thus, the IR cell was not considered a significant source of air or moisture contamination.

^{1}H NMR experiments

An NMR tube with a screw-cap septum top was first filled with solvent and aniline in a nitrogen filled dry box to and then the ^{1}H NMR spectrum was obtained. After this initial ^{1}H NMR analysis, the NMR tube was returned to the dry box, and the solution was transferred to a vial for CuCl addition. Then, the solvent-aniline-CuCl solution was transferred back into the NMR tube and analyzed. Next, ethylene gas with a flow rate of >50 ml/min was added to the NMR tube under a fume hood for 2 min. This process of adding ethylene was performed twice, and after ethylene addition, the solution was stored under the atmosphere of ethylene for approximately 1 h before ^{1}H NMR analysis. The same procedure was repeated for an NMR tube filled with only solvent. This sample was tested to provide a comparison between complexed and uncomplexed ethylene.

Table 3 below lists the solutions analyzed using ^{1}H NMR spectroscopy. Note that NMR Solutions 1, 2, and 3 and NMR Solution 5, 6, and 7 are synthesized in a single tube with consecutive additions of reagents.

The first ^{1}H NMR tests used CD_3OD to investigate the feasibility of ^{1}H NMR spectroscopy, as methanol contains fewer functional groups that could complicate spectral analysis. After successful results with CD_3OD, the tests moved to using deuterated dimethylformamide (DMF-d_7). ^{1}H NMR spectra were recorded using a Varian Gemini (300 MHz) spectrometer. Chemical shifts are reported in delta (δ) units and expressed in parts per million (ppm) downfield from tetramethylsilane using the residual protio solvent as an internal standard (3.31 ppm for CD_3OD and 2.92 ppm for DMF-d_7).[44]

Results and Discussion

Preliminary experiments

The crystallization experiment was conducted twice as mentioned previously. During the first experiment, the solution was black–green at low temperatures (−15°C) and black–brown at room temperature (25°C). This color change was replicated by repeating the chilling–warming cycle. At low temperatures, a white residue was obtained at the bottom of the flask. This residue remained at room temperature, though in reduced quantity, in the form of a viscous fluid. After a week at room temperature, the residue dissolved into the solution and the color change could not be reproduced with temperature shifts.

In the second experiment, the solution exhibited similar color characteristics, but generated lesser amounts of residue. At room temperature, the residue was not observable. Figures 12 and 13 below illustrate the color changes between temperatures, whereas Figure 14 shows the presence of residue. All pictures were of the second experiment.

The green color at cold conditions suggests presence of Cu(II). This impurity was likely present in the Cu(I) starting material, as the powder right out of the bottle displayed a greenish hue. Although the source of the brown color at room conditions remains unknown, the color change likely indicates a change in coordination. Thus, the temperature most likely affects the structures formed in solution. The black color of the solution was attributed to oxidation impurities as the solutions made in the dry box for the IR and ^{1}H NMR experiments were green and somewhat translucent. Finally, the presence of residue in the preliminary experiments was most likely undissolved CuCl, though the identity of the residue remains unknown. The dissolution of the residue after a week supports this conclusion. Thus, the preliminary experiments suggest that for this system, crystallization is unlikely for temperatures as low as −15°C.

Table 3. ^{1}H-NMR Solutions

Name	CD_3OD	DMF-d_7	Aniline	CuCl	Ethylene (138 kPa)	CuCl Conc.	Aniline:CuCl Molar Ratio
NMR solution 1	1 mL	~	0.182 mL	~	No	~	~
NMR solution 2	1 mL	~	0.182 mL	100.8 mg	No	1 M	2:1
NMR solution 3	1 mL	~	0.182 mL	100.8 mg	Yes	1 M	2:1
NMR solution 4	1 mL	~	~	~	Yes	~	~
NMR solution 5	~	1.06 mL	0.18 mL	~	No	~	~
NMR solution 6	~	1.06 mL	0.18 mL	98 mg	No	0.92 M	2.03:1
NMR solution 7	~	1.06 mL	0.18 mL	98 mg	Yes	0.92 M	2.03:1
NMR solution 8	~	1.06 mL	~	~	Yes	~	~

Figure 12. Black–green solution at −15°C.

[Color figure can be viewed in the online issue, which is available at wileyonlinelibrary.com.]

IR experiments

Several qualitative observations were made during the preparation of the IR solutions described in Tables 1 and 2 above. During the preparation of IR Solution 2, the solution displayed a transparent light green color. On addition of ethylene in IR Solution 3, no visible changes were observed. However, during the loading of IR Solution 3 into the IR cell, large gas bubbles were observed in the IR cell. As gas bubbles were not observed in the other two tests, this was assumed to be ethylene released by the solution. Finally, during the preparation of IR Solution 5, the solution color changed from a light green color to a black–red color over the span of a few minutes. This was deemed to be an effect of air contamination of the Cu(I) ion.

Figure 13. Black–brown solution at 25°C.

[Color figure can be viewed in the online issue, which is available at wileyonlinelibrary.com.]

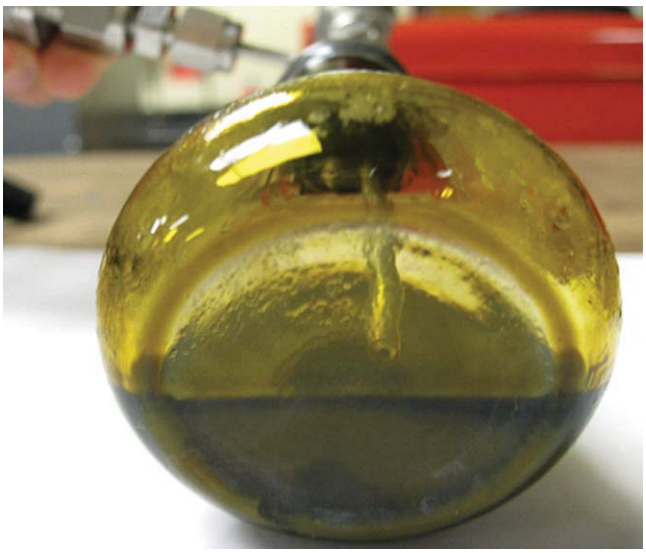

Figure 14. Residue at −15°C.

[Color figure can be viewed in the online issue, which is available at wileyonlinelibrary.com.]

All solutions in NMP displayed significant interference from the absorption bands of the solvent. NMP absorbs strongly in the following ranges: 2800–3000 cm^{-1} due to C—H stretching, 1650–1750 cm^{-1} due to C=O stretching, 1400–1500 cm^{-1} due to C—N stretching and C—H bending, and 1200–1300 cm^{-1} due to C(methyl)—N stretching.[45] Unfortunately, strong solvent absorption makes proper baseline subtraction difficult. This interference obscured or eliminated many areas of interest and caused extensive noise in the solution spectra, especially in the low frequency range. Thus, due to excessive interference, important metal-nitrogen and metal-chloride interactions could not be studied. However, certain peaks did appear with acceptably low levels of interference, which allowed for analysis. The IR data gathered for the solutions in NMP are shown below in Table 4. The peaks were assigned by comparing the experimental data with a standard.[45]

In IR Solution 1, the vibrations for the N—H functional group and aromatic ring agreed well with literature, though the shoulder peak at 3237 cm^{-1} exhibited much stronger

Table 4. IR Data for NMP

	Verified Peaks		
Solution Name	Wavenumber (cm^{-1})	Functional Group	Vibration Mode
IR solution 1: NMP + $PhNH_2$	3421	N—H	Asymm stretch
	3347	N—H	Symm stretch
	3237	N—H	Bend (overtone)
	1602	C=C (Ar)	Stretch
IR solution 2: NMP + $PhNH_2$ + CuCl	3422	N—H	Asymm stretch
	3346	N—H	Symm stretch
	3236	N—H	Bend (overtone)
	1631	N—H	Bend
	1603	C=C (Ar)	Stretch
IR solution 3: NMP + $PhNH_2$ + CuCl + ethylene	3422	N—H	Asymm stretch
	3346	N—H	Symm stretch
	3236	N—H	Bend (overtone)
	1631	N—H	Bend
	1603	C=C (Ar)	Stretch

Table 5. IR Data for MeOH

Solution Name	Verified Peaks		
	Wavenumber (cm^{-1})	Functional Group	Vibration Mode
IR Solution 4:	1630	N—H	Bend
MeOH + $PhNH_2$	1602	C=C (Ar)	Stretch
	1496	C=C (Ar)	Stretch
	1271	C—N	Stretch
IR Solution 5:	1631	N—H	Bend
MeOH +	1606	C=C (Ar)	Stretch
$PhNH_2$ + CuCl	1496	C=C (Ar)	Stretch
	1263	C—N	Stretch

absorbance and the aromatic peak ~1500 cm^{-1} was eliminated by over-subtraction.[45,46] Surprisingly, the addition of CuCl in IR Solution 2 did not produce the shifts documented by literature. The only observable change was a slight decrease in the frequency of the N—H bend by approximately ~10 cm^{-1}. This decrease is slightly less than the shift values found in literature and could be a result of errors incurred during peak smoothing. Thus, assuming that aniline is coordinating with CuCl, these data indicate that coordination with CuCl does not affect the force constants of N—H. This also suggests that the amine nitrogen coordinates weakly with CuCl and does not donate much electron density to Cu(I) in these solutions.

On addition of ethylene in IR Solution 3, no ethylene peak was observed and the spectra remained essentially unchanged from IR Solution 2. This was likely due to the release of ethylene during cell loading, as noted above. Also, due to the strong absorption of NMP in the region where the ethylene peak was found, the entire area was eliminated by oversubtraction. Thus, with these two effects, no ethylene peak was observed.

In an attempt to reduce solvent interference, methanol was substituted for NMP to make IR Solutions 4 and 5. Because of the complications of ethylene addition as noted above, ethylene was not added to the methanol solutions. Unfortunately, both spectra still exhibited significant interference, though less than that found in the NMP spetra. The IR data for the methanol solutions are shown below in Table 5.

Both IR Solutions 4 and 5 displayed a multitude of peaks in the approximate frequency range of N—H stretching vibrations. However, the number and shape of the peaks do not resemble those found in literature, and it is unclear whether these can be assigned as N—H stretch peaks. The source of this interference may be incorrect subtraction of the highly variable methanol O—H. Nevertheless, the frequencies of other vibrational modes of aniline in IR Solution 4 agreed well with literature. The addition of CuCl again caused little change in the verified peaks, except for ~10 cm^{-1} decrease in frequency of the C—N stretch. These results reinforce the hypothesis of a weak aniline-Cu(I) interaction.

^{1}H NMR experiments

Several qualitative observations were made during the synthesis of the NMR solutions described in Table 3 above. During the preparation of NMR Solution 2, the solution took on a brown color and a significant amount of fluffy brown precipitate formed. On addition of ethylene (NMR Solution 3), the brown precipitate was reduced in quantity, became darker in color, and lost its fluffy appearance. During the synthesis of NMR Solution 6, the solution took on an opaque light-green appearance, with a whitish residue on the bottom resembling that found in the preliminary experiments. Addition of ethylene did not affect this residue. The precipitate in both solvents may be excess CuCl rendered insoluble due to the smaller aniline:Cu(I) ratio and higher Cu(I) concentrations used in the NMR experiments as compared with the preliminary experiments and the IR experiments. However, the visual discrepancies in the precipitates of the two solvent systems require further analysis to verify this hypothesis. Finally, in the synthesis of NMR Solution 7, the formation of a thin black film at the vapor-solution interface was observed. This was attributed to air contamination, as the insertion of the syringe needles during ethylene addition may have caused a small leak. However, as the bulk solution remained unchanged, the effect of this was deemed negligible.

The ^{1}H NMR data gathered from tests in deuterated methanol (CD_3OD) are shown below in Table 6. Note that *o*, *p*, and *m* represent ortho, para, and meta aromatic hydrogens, respectively. Also, the approximate shifts for the aromatic hydrogens are calculated by taking the midpoint between the

Table 6. ^{1}H-NMR Data for CD_3OD

Solution Name	Observations			
	Chemical Shift (# of H)	Functional Group	Splitting	Peak Width
NMR solution 1:	4.857 (2)	N—H	No	Broad
CD_3OD + $PhNH_2$	~6.70 (3)	Ar—H (*o* and *p*)	Yes	Sharp
	~7.09 (2)	Ar—H (*m*)	Yes	Sharp
NMR solution 2:	4.805 (2)	N—H	No	Broad
CD_3OD + $PhNH_2$ + CuCl	~6.85 (3)	Ar—H (*o* and *p*)	Yes (less)	Slightly broad
	~7.089 (2)	Ar—H (*m*)	Yes (less)	Slightly broad
NMR Solution 3:	4.808 (2)	N—H	No	Broad
CD_3OD + $PhNH_2$ + CuCl + C_2H_4	~6.71 (3)	Ar—H (*o* and *p*)	Yes	Sharp
	~7.09 (2)	Ar—H (*m*)	Yes	Sharp
	4.663 (0.32)	C=C—H	No	Sharp
NMR solution 4:	~3.00 (3)	C—D (methanol)[46]	Yes	Sharp
CD_3OD + C_2H_4	4.863 (1.64)	O—D (methanol)[46]	No	Sharp
	5.361 (NA)	C=C—H	No	Sharp
	5.376 (NA)	C=C—H	No	Sharp

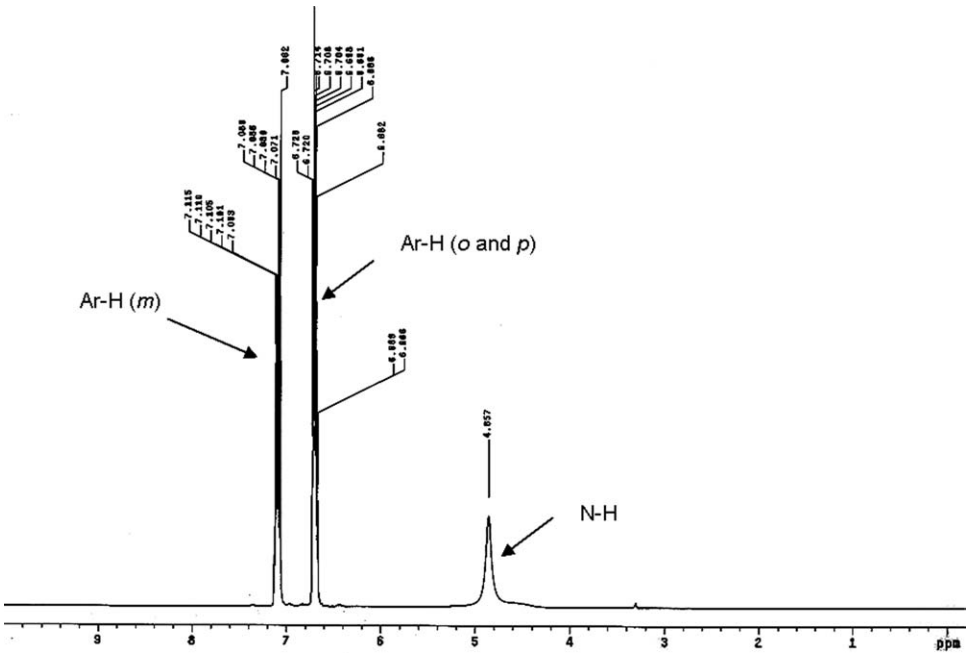

Figure 15. 1H NMR graph of CD_3OD and aniline.

lowest and highest peak in the multiplet. Figure 15 shows the graph of NMR Solution 1.

The graph displays a broadened singlet for the N—H bonds at 4.857 ppm, indicating a large quadrupole moment and equivalent states for all amine hydrogens.[30] On the other hand, the peaks for the aromatic hydrogens exhibit extensive peak splitting. The peaks for the ortho and para hydrogens are partially overlapped, indicating similar magnetic environments for the two species of hydrogens.

On addition of CuCl (NMR Solution 2), the N—H peak shifts upfield by 0.052 ppm to 4.805 ppm. Figure 16 illustrates this upfield shift. Notably, this disagrees with the downfield shifts generally observed in literature. However, the peak shift is small, which suggests that the amine nitrogen does not donate significant electron density to the metal center. Also, the addition of CuCl causes the aromatic hydrogen peaks to broaden slightly and reduce peak splitting, which leads to the complete overlap of the ortho and para hydrogens. This broadening may be caused by coordination through the amine nitrogen and subsequent changes in resonance. Another possibility may be the interaction suggested by Ruan et al. through a single π-bond in the aromatic ring.[9]

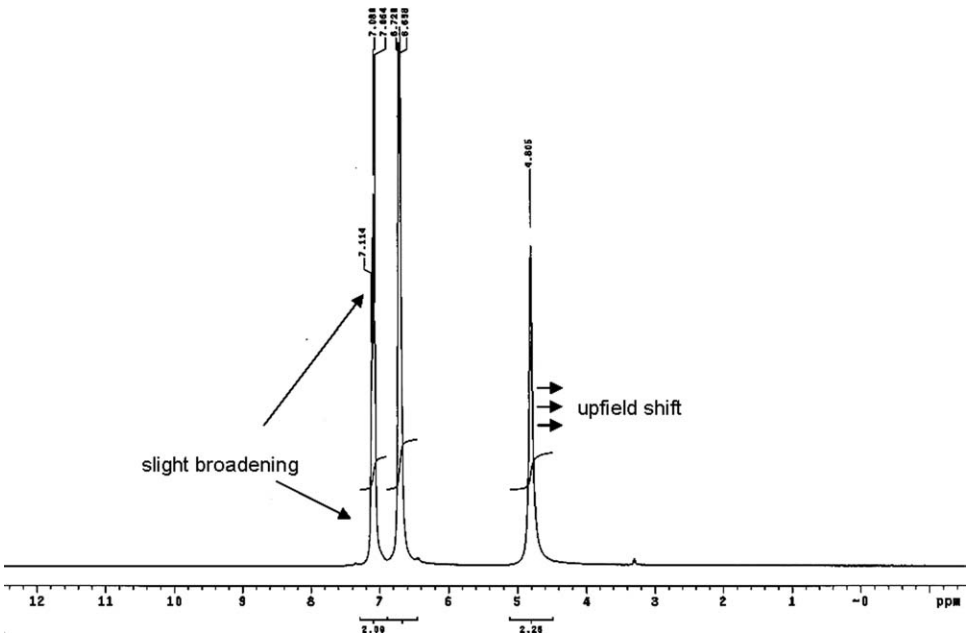

Figure 16. 1H NMR graph of CD_3OD, aniline, and CuCl.

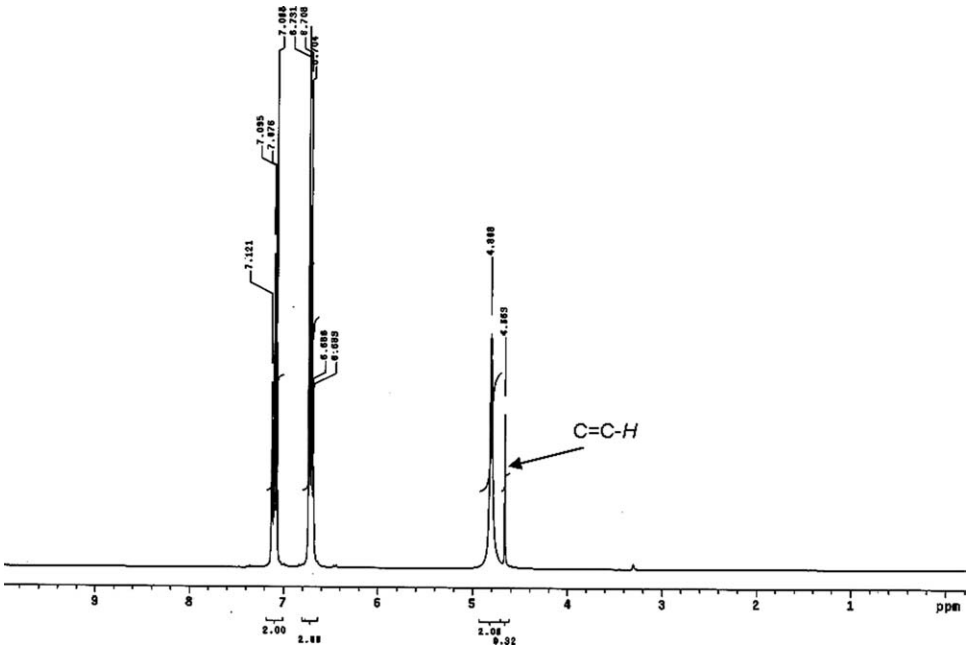

Figure 17. 1H NMR graph of CD_3OD, aniline, CuCl, and ethylene.

Adding ethylene to the solution (NMR Solution 3) causes another peak to appear at 4.663 ppm, which was assigned to the C═C—*H* functional group from ethylene, as shown by Figure 17. The area of this peak (0.32 H) should qualitatively indicate the amount of ethylene absorbed. Even so, it is unknown whether this area can be related to the coordination number of ethylene due to the fast exchange of complexed ethylene with free ethylene. The N—H peak changes little in shift or width, indicating a minimal effect of ethylene on aniline complexation. However, the aromatic hydrogen peaks sharpen and regain peak splitting characteristics. The reason for this effect remains unexplored.

Using the shift of the ethylene peak in NMR Solution 4, the upfield shift of the ethylene hydrogens due to complexation was calculated to be 0.713 ppm (5.376 to 4.663 ppm). The direction and magnitude of this upfield shift as well as the position of the ethylene peak agrees roughly with the relation between ligand basicity and ^{1}H NMR shift established in literature.[8,34] Still, given a pKa of 4.63 for aniline, the chemical shift is approximately 0.58 ppm greater than that found by Munakata et al.[8,27] This result indicates that greater π-backbonding occurs in this system. As the shifts in literature were recorded in acetone-d_6, the increased upfield shift observed in CD_3OD may be an effect of increased solvent polarity. Finally, in NMR solution 4, two C═C—H singlets are observed and are separated by 0.005 ppm. The reason for this effect also remains unexplored, though the minute difference may be a result of NMR error.

Table 7 below summarizes the data from the ^{1}H NMR tests in deuterated dimethylformamide (DMF-d_7). Figure 18 shows the graph of NMR Solution 5. In this graph, again the N—H functional group displayed a single broad peak, whereas the

Table 7. ^{1}H-NMR Data for DMF-d7

	Observations			
Solution Name	Chemical Shift (# of H)	Functional Group	Splitting	Peak Width
NMR solution 5:	5.197 (2)	Ar—N—H	No	Broad
DMF-d7 + $PhNH_2$	~6.88 (2)	Ar—H (*o*)	Yes	Sharp
	~6.73 (1)	Ar—H (*p*)	Yes	Sharp
	~7.23 (2)	Ar—H (*m*)	Yes	Sharp
NMR solution 6:	~	Ar—N—H	No	Very broad
DMF-d7 + $PhNH_2$ + CuCl	6.95 (2)	Ar—H (*o*)	No	Broad
	6.802 (1)	Ar—H (*p*)	No	Broad
	7.365 (2)	Ar—H (*m*)	No	Broad
NMR solution 7:	~	Ar—N—H	~	Flat
DMF-d7 + $PhNH_2$ + CuCl + C_2H_4	6.743 (3)	Ar—H (*o* and *p*)	Yes	Very broad
	7.434 (2)	Ar—H (*m*)	No	Broad
	4.384 (NA)	C═C—H	No	Sharp
NMR solution 8:	~2.91 (3)	C—H (DMF)[46]	Yes	Sharp
DMF-d7 + C_2H_4	~3.09 (3)	C—H (DMF)[46]	Yes	Sharp
	8.192 (1)	O═C—H (DMF)[46]	No	Sharp
	5.57	C═C—H	No	Sharp
	5.577	C═C—H	No	Sharp

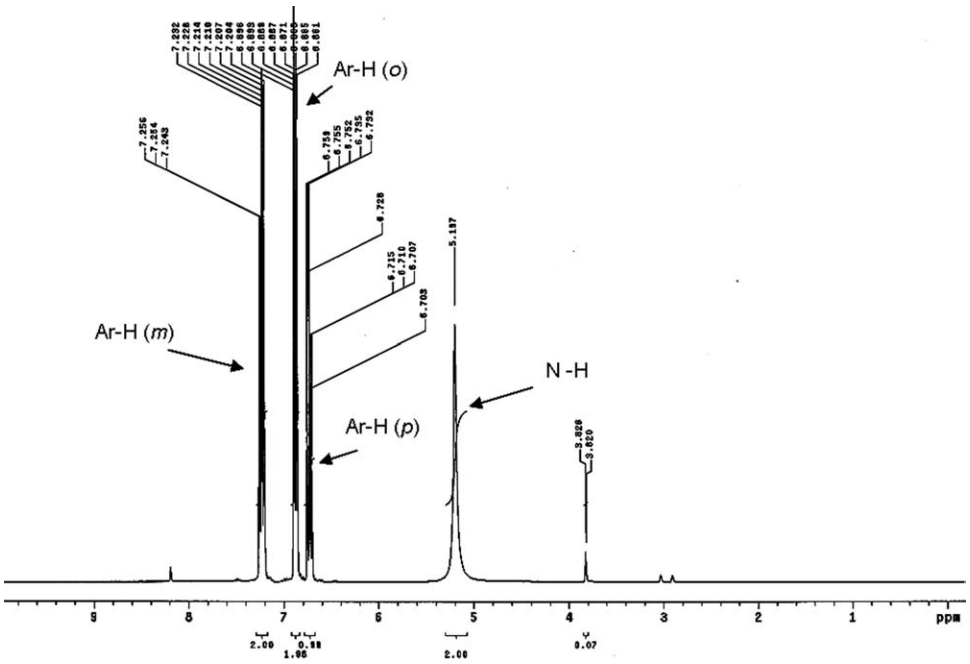

Figure 18. 1H NMR graph of DMF-d_7 and aniline.

aromatic hydrogens resolved into sharp multiplets. However, the N—H peak in DMF-d_7 resonates 0.34 ppm farther downfield than the N—H peak in CD_3OD. The ortho and meta aromatic hydrogen peaks also move downfield 0.18 ppm and 0.14 ppm, respectively, but the para aromatic peak only moves 0.03 ppm downfield. The downfield shifts of the amine hydrogens, the ortho aromatic hydrogens, and the meta aromatic hydrogens result from interactions between aniline and DMF-d_7. The oxygen on the carbonyl group acts as a hydrogen bond acceptor while the aniline N—H group acts as a hydrogen bond donor.[47] This positions the hydrogen in the N—H group in the deshielding region of the carbonyl group's anisotropic field,[30] thus shifting the amine hydrogens downfield. As the amine hydrogens are the closest to the carbonyl group, they exhibit the largest amount of shift, as the amount of deshielding varies inversely with distance.[30] Thus, the distance of the aromatic hydrogens from the carbonyl group (ortho < meta < para) predicts the amount of downfield shift (0.18 ppm, 0.14 ppm, 0.03 ppm). Because CD_3OD does not possess an anisotropic field, this effect is not seen in the ^{1}H NMR graphs with CD_3OD as the solvent. Finally, the ^{1}H NMR graph of NMR Solution 5 also shows a small doublet at ~3.823 ppm which is most likely results from water contamination.[44]

On addition of CuCl (NMR Solution 6), a dramatic broadening of all peaks occurs, especially for the amine hydrogens. Figure 19 shows illustrates this effect. The N—H peak broadens until it becomes only a wide hump from approximately 3.2 ppm to 6.4 ppm, whereas the aromatic hydrogen peaks broaden significantly and lose all peak splitting characteristics. The broadening also causes the ortho and para aromatic hydrogen partially overlap. These effects cannot be entirely explained by complexation with Cu(I), as broadening is not seen with CD_3OD, nor can it be entirely explained by the change in solvent since broadening is not seen without CuCl. One explanation may be that the increase in the dielectric constant of the solvent produces stronger aniline–solvent interactions, slowing the exchange rate of coordinated and uncoordinated aniline from a fast exchange rate to an intermediate exchange rate. This would cause the observed flattening and broadening of the peak. Another contributing factor may be the variability of the coordination number around the Cu(I) ion due to the lability of the aniline-Cu(I) complex, as the number and species of ligands attached to Cu(I) should change the surrounding magnetic environment. Although this effect by itself does not seem to cause line broadening in CD_3OD, if combined with the slower exchange of aniline in DMF-d_7, greater line broadening may occur. Finally, because both the amine peak and the aromatic hydrogen peaks are broadened, aniline may be coordinating through the aromatic ring as well as the nitrogen atom, as mentioned previously. Further studies are required to verify the validity of these hypotheses.

Figure 20 shows the ^{1}H NMR graph upon addition of ethylene (NMR Solution 7). Adding ethylene to the solution (NMR Solution 7) yields an additional ethylene peak at 4.384 ppm with an area of 0.31 H. Also, the amine hydrogen peak disappears while the aromatic hydrogen peaks broaden even further, the latter causing the ortho and para aromatic hydrogen peaks to almost completely overlap. The addition of ethylene in DMF-d_7 may cause further peak broadening due to its labile interaction with Cu(I), which would increase the differences between magnetic states by increasing the number of ligand species coordinating with Cu(I). However, the ^{1}H NMR data taken in CD_3OD displays peak sharpening, which argues the opposite effect of ethylene complexation. This contradiction reaffirms the complexity of this system, and further study is needed to clarify these observations.

Using the shift of the ethylene peak in NMR Solution 8 (5.57 ppm), the upfield shift of the ethylene hydrogens due to complexation was calculated to be 1.186 ppm. The

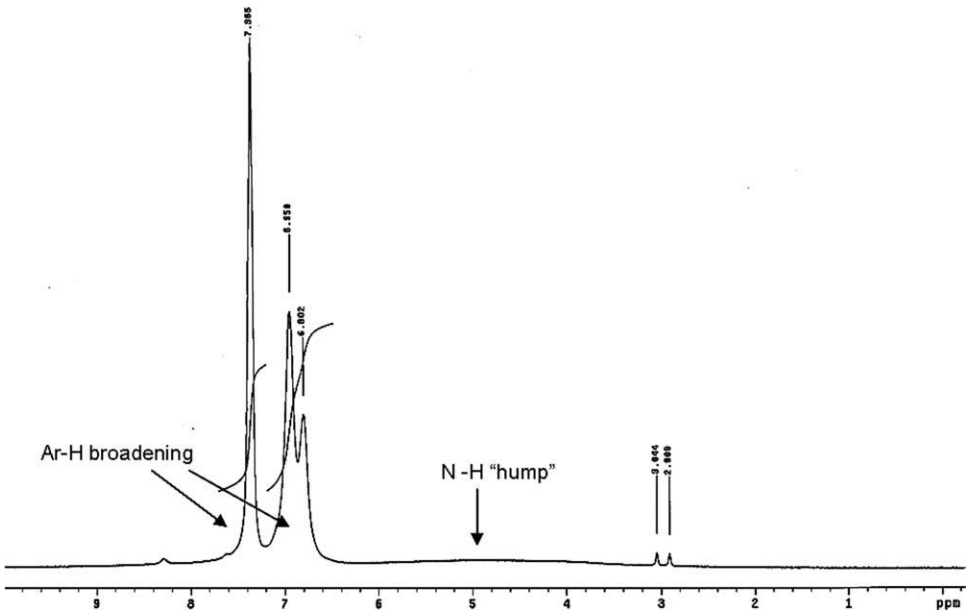

Figure 19. 1H NMR graph of DMF-d_7, aniline, and CuCl.

increase in upfield shift of 0.713 ppm to 1.186 ppm by changing the solvent indicates that DMF-d_7 promotes greater π backbonding than CD_3OD. Also, since DMF-d_7 is more polar than CD_3OD, this result supports the hypothesis proposed previously on the direct relation between solvent polarity and the upfield shift of complexed ethylene. Finally, in NMR Solution 8, two C═C─H singlets appear, separated by 0.007 ppm, whereas a water peak appears at 3.548 ppm.

Conclusions

This research project explored the structural characteristics of a Cu(I)-based absorption solution with ethylene to aid future development of olefin–paraffin separation systems. Because of the structural clarity afforded by X-ray crystallography, a preliminary experiment was designed to investigate the feasibility of crystallization. Unfortunately, a lack of precipitation at attainable temperatures indicated that crystallization of a CuCl-aniline-ethylene complex lay out of reach. Although a residue formed at cold temperature, its identity was likely undissolved CuCl. However, these experiments did reveal a temperature-dependent coordination as well as the aesthetic effects of air contamination. The black discoloration caused by air and copper points to copper oxide formation, and this color change can be used to identify the presence of air in the system.

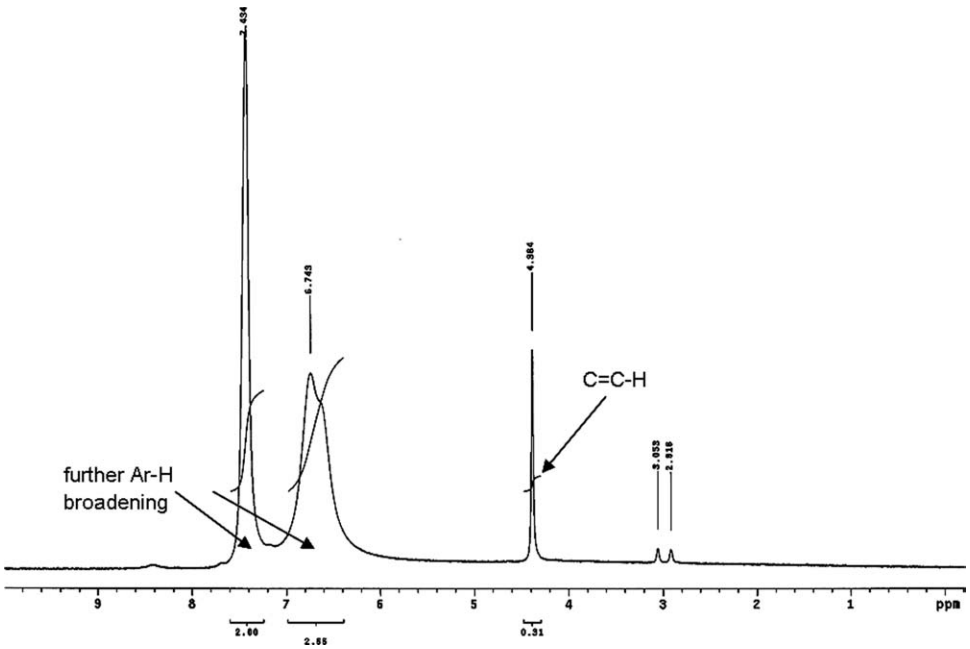

Figure 20. 1H NMR graph of DMF-d_7, aniline, CuCl, and ethylene.

Next, this study investigated Cu(I)-ethylene and Cu(I)-aniline coordination by analyzing the solution using infrared spectroscopy. Surprisingly, the addition of CuCl to a solution of aniline and solvent produced very little change in aniline vibrations. As coordination would seemingly induce electron donation from aniline to copper and cause changes in force constants, these data indicate a very weak aniline-Cu(I) coordination. Unfortunately, problems prohibited further analysis using IR spectroscopy. First, complications arose from the choice of solvent system. The multitude of functional groups on NMP caused excessive solvent interference during baseline subtraction. Thus, large areas of oversubtraction and undersubtraction obscured many peaks of interest, while noisy spectra impeded analysis of other frequency ranges. Notably, the excessive noise in the low frequency prohibited any recognition of metal-nitrogen and metal-chloride vibrations. Changing the solvent to MeOH reduced interference, but interference with the N—H stretch vibrations occurred. The use of a nonpolar solvent with few functional groups would aid in infrared analysis but may also cause solubility issues with aniline and CuCl. In addition to solvent complications, the IR spectra of the ethylene-containing solution failed to produce any identifiable ethylene vibrations. This obscuration likely arose from the escape of ethylene during cell-loading as well as oversubtraction of the area of interest. Given these difficulties, infrared spectroscopy proved to be an unsatisfactory characterization method, as it may require specialized equipment such as a high pressure IR cell.

^{1}H NMR spectroscopy showed much more promise as an analytical technique. The spectrum of a solution containing aniline and deuterated methanol (CD_3OD) clearly displayed the characteristic resonances of aniline. Adding CuCl to this solution caused slight line broadening, an effect most likely due to coordination. Also, since line broadening occurred with both the aromatic ring resonances and the aniline resonances, coordination may occur through a single π-bond in the aromatic ring as well as the nitrogen atom. However, the shift of the resonances changed very little, further reinforcing the hypothesis of weak aniline complexation. Addition of ethylene to the above solution caused a clear, sharp singlet to appear at 4.663 ppm, which suggests a fast, labile coordination of ethylene. The ethylene peak also shifted upfield by 0.713 ppm from free ethylene in CD_3OD (5.376 ppm), a greater upfield shift than that found in literature. The increased polarity of the NMR solvent (CD_3OD vs. acetone-d_6) may be the cause of the greater shift, though this hypothesis remains untested. Notably, the addition of ethylene did not affect the shifts of the aniline resonances, though it did reduce line broadening. Finally, the spectrum of pure ethylene in CD_3OD displayed two ethylene peaks, which may indicate the differences in dissolved and free ethylene.

The ^{1}H NMR spectra of solutions with deuterated dimethylformamide (DMF-d_7) displayed significant differences from those taken in CD_3OD. The addition of CuCl again does not change the shifts of aniline resonances, but causes drastic line broadening. In fact, the amine resonance changes from a singlet to a wide hump spanning 3.2 ppm to 6.4 ppm. The higher dielectric constant of DMF may produce stronger aniline–solvent interactions, slowing the exchange rate of coordinated and uncoordinated aniline. Given the differences in magnetic environment caused by coordination as well as variations in the coordination number of aniline, slowing the exchange from a fast rate to an intermediate rate would cause line broadening. Although this hypothesis remains unproven, neither the addition of CuCl nor the change of solvent alone can cause extensive line broadening. This reveals that solvent choice greatly affects the coordination of aniline to Cu(I). The addition of ethylene to the solution of aniline, CuCl, and DMF-d_7 causes a sharp singlet to appear at 4.384 ppm, which is 1.185 ppm upfield of free ethylene in DMF-d_7 (5.57 ppm). The larger upfield shift indicates that DMF-d_7 promotes greater π-backbonding than CD_3OD, and reinforces the hypothesis of the direct relation between solvent polarity and upfield shift. Also, ethylene addition slightly increases line broadening, an effect that contradicts the reduction in broadening found in CD_3OD. This disagreement was also left uninvestigated. Finally, the spectrum of pure ethylene in DMF-d_7 also exhibited two peaks, which may be explained by reasons detailed previously.

Notably, the preparation of the solutions for IR and NMR characterization revealed several interesting behaviors. First, the IR solutions with methanol were prepared in a fume hood, and thus, air and moisture contamination occurred. During the addition of aniline to a mixture of CuCl and methanol, the solution turned from light green to black–red over the span of several minutes, indicating a fast timescale of contamination. Second, during the synthesis of the NMR solutions, addition of CuCl produced a fluffy brown precipitate in CD_3OD and a white residue in DMF-d_7. Addition of ethylene affected the former but not the latter. Although the precipitate may be uncomplexed CuCl, the differences in appearance and behavior between the CD_3OD precipitate and the DMF-d_7 precipitate suggest otherwise. Characterization of these precipitates may yield structural information about the CuCl-aniline-ethylene system as well as the effect of solvent differences.

In summary, the CuCl-aniline-ethylene system exhibits weak and labile aniline and ethylene complexation. Furthermore, the agreement of the spectral data with mono-ethylene complexes suggests single ethylene coordination. Unfortunately, the coordination of the Cl^- ion could not be investigated, though it most likely remains coordinated to the Cu(I) ion. Although the solvent molecules may not coordinate with the Cu(I) ion, solvent–ligand interactions play a large role in complexation. Finally, due to the lability of ethylene and aniline, assignment of any single coordination structure should be resisted, as multiple structures probably coexist in solution.

The absorption solution with aniline exhibits optimal ethylene capacities most likely due to weaker competition for coordination sites compared with other, stronger ligands. However, a tradeoff should exist between ethylene capacity and complex stability. Because of the equilibrium-controlled nature of these interactions, any impurity with a larger equilibrium constant toward complexation other than aniline or ethylene would likely poison the copper. A ligand that would prefer complexation would also be more likely to block ethylene from coordination. Thus, an optimal ligand must be found that balances ethylene capacity and degradation resistance.

Literature Cited

1. Smith JM, Van Ness HC, Abbott MM. *Appendix B*. In: *Introduction to Chemical Engineering Thermodynamics*, *7th ed*. Boston: McGraw-Hill, 2005:680.

2. Astruc D. *Organometallic Chemistry and Catalysis*. New York: Springer, 2000.
3. Reine TA, Eldridge RB. Absorption equilibrium and kinetics for ethylene-ethane separation with a novel solvent. *Ind Eng Chem Res*. 2004;44:7505–7510.
4. Reine TA, Eldridge RB. Use of electrochemistry to predict ethylene absorption capacities of reactive absorption systems. *Ind Eng Chem Res*. 2004;43:6514–6520.
5. Safarik DJ, Eldridge RB. Olefin/separations by reactive absorption: a review. *Ind. Eng Chem Res*. 1998;37:2571–2581.
6. Chen JP, Yang RT. A molecular orbital study of the selective adsorption of simple hydrocarbon molecules on Ag+- and Cu+ exchanged resins and cuprous halides. *Langmuir*. 1995;11: 3450–3456.
7. Dias HR, Wu J. Structurally characterized coinage-metal-ethylene complexes. *Eur J Inorg Chem*. 2008;4:509–522.
8. Munakata M, Kitagawa S, Kosome S, Asahara A. Studies of copper(I) olefin complexes. Formation constants of copper olefinComplexes with 2,2′-bipyridine, 1,10-phenanthroline, and their derivatives. *Inorg Chem*. 1986;25:2622–2627.
9. Ruan C, Yang Z, Rodgers MT. Influence of the d orbital occupation on the nature and strength of copper cation-pi interactions: threshold collision-induced dissociation and theoretical studies. *Phys Chem Chem Phys*. 2007;9:5902–5918.
10. Thompson JS, Swiatek RM. Copper(I) complexes with unsaturated small molecules. Synthesis and properties of monoolefin and carbonyl complexes. *Inorg Chem*. 1985;23:110–113.
11. Suenaga Y, Wu LP, Kuroda-Sowa T, Munakata M, Maekawa M. Structure and HNMR study of copper(I) complex with ethylene and tetramethylethylenediamine. *Polyhedron*. 1997;16:67–70.
12. Dias HR, Fianchini M, Cundari TR, Campana CF. Synthesis and characterization of the gold(I) tris(ethylene) complex [Au(C2H4)3][SbF6]. *Angew Chem Int Ed Engl*. 2008;47:556–559.
13. Flores JA, Dias HR. Gold(I) ethylene and copper(I) ethylene complexes supported by a polyhalogenated triazapentadienyl ligand. *Inorg Chem*. 2008;47:4448–4450.
14. Huang HY, Padin J, Yang RT. Comparison of pi-Complexations of ethylene and carbon monoxide with Cu+ and Ag+. *Ind Eng Chem Res*. 1999;38:2720–2725.
15. Tai H-C, Krossing I, Seth M, Deubel DV. Organometallics versus P4 complexes of group 11 cations: periodic trends and relativistic effects in the involvement of (*n*-1)d, ns, and np orbitals in metal-ligand interactions. *Organometallics*. 2004;23:2343–2349.
16. Ho WW, Doyle G, Savage DW, Pruett RL. Olefin separations via complexation with cuprous diketonate. *Ind Eng Chem Res*. 1988;27:334–337.
17. Cotton FA, Wilkinson G, Gaus PL. *Basic Inorganic Chemistry*. New York: Wiley, 1995.
18. Zaklika KA, Thayer AL, Schaap AP. Interaction of an aliphatic C-H bond with copper in a norbornene(diethyltriamine)copper(I) cation complex. *J Am Chem Soc*. 1978;100:4918–4919.
19. Dai X, Warren TH. Dioxygen activation by a neutral beta-diketiminato copper(I) ethylene complex. *Chem Commun*. 2001;19: 1998–1999.
20. Straub BF, Eisentrager F, Hoffman P. A remarkably stable copper(i) ethylene complex: synthesis, spectroscopy and structure. *Chem Commun*. 1999;2507–2508.
21. Thompson JS, Calabrese JC, Whitney JF. Copper (I)-olefin complexes. Structure of (1-2-u-cyclohexene)-(di-2-pyridylamine)copper(I) perchlorate, [Cu(C6HI0)(C10H9N3)]CIO4*. *Acta Cryst*. 1985; 41:890–892.
22. Thompson JS, Harlow RL, Whitney JF. Copper(I)-olefin complexes. Support for the proposed role of copper in the ethylene effect in plants. *J Am Chem Soc*. 1983;105:3522–3527.
23. Wang X-S, Zhao H, Li Y-H, Xiong R-G, You X-Z. Olefin-copper(I) complexes and their properties. *Topics Catalysis*. 2005;35(1–2): 43–61.
24. Hirsch J, George SD, Solomon EI, Hedman B, Hodgson KO, Burstyn JN. Raman and extended x-ray absorption fine structure characterization of a sulfur-ligated Cu(I) ethylene complex: modeling the proposed ethylene binding site of Arabidopsis thaliana ETR1. *Inorg Chem*. 2001;40:2439–2441.
25. Sullivan RM, Lu H, Smith DS, Hanson JC, Osterhout D, Ciraolo M, Grey CP, Martin JD. Sorptive reconstruction of the CuAlCl4 framework upon reversible ethylene binding. *J Am Chem Soc*. 2003;125: 11065–11079.
26. Santiso-Quinones G, Reisinger A, Slattery J, Krossing I. Homoleptic Cu-phosphorus and Cu-ethene complexes. *Chem Commun*. 2007; 47:5046–5048.
27. Munakata M, Kitagawa S, Shimono H, Masuda H. Synthesis, characterization, and molecular structures of binary and ternary copper(I) complexes with 1,5-cyclooctadiene (cod): [Cu(cod)2]ClO4 and [cu(cod)(2,2′-bipyridine)]PF6. *Inorg Chem*. 1991;30:2610–2614.
28. Labanowska M, Zurowski KR, Bidzinska E. Electron paramagnetic resonance investigations of ammonia and aniline copper (II) complexes. *Colloids Surfaces*. 1996;115:297–301.
29. Sunderrajan S, Freeman BD, Hall CK. Fourier transform infrared spectroscopic characterization of olefin complexation by silver salts in solution. *Ind Eng Chem Res*. 1999;38:4051–4059.
30. Pavia DL, Lampman GM, Kriz GS, Vyvyan JR. *Introduction to Spectroscopy*, *4th ed*. USA: Brooks/Cole Cengage Learning, 2009.
31. Malik AU. Coordination compounds of cuprous iodide with heterocyclic amines. *J Inorg Nuclear Chem*. 1967;29:2106–2107.
32. Prasad S, Trivedi SR. Complexes of cuprous bromide with secondary and tertiary amines and heterocyclic bases in nonaqueous media. *J Institution Chemists*. 1968;40:9–14.
33. Akalin E, Akyuz S. Force field and IR intensity calculations of aniline and transition metal(II) aniline complexes. *J Mol Structure*. 1999;482–483:175–181.
34. Akyuz S. An infrared spectroscopic study of dianiline-metal(II) tetracyanometalate complexes. *J Mol Structure*. 1980;68:41–49.
35. Craciunescu D, Oancea D. Molecular structure of the new copper complexes. VIII. Infrared spectroscopic evidence of the Cu2+ ion interaction with aniline derivates (chloro and nitroanilines). *Israel J Chem*. 1970;8:581–587.
36. Lee-Thorp JA, Ruede JE, Thornton DA. The infrared spectra (3500–150 cm^{-1}) of aniline complexes of cobalt(II), nickel(II), copper(II) and zinc(II) halides. *J Mol Structure*. 1978;50:65–71.
37. Akyuz S, Davies JE. Solid-state vibrational spectroscopy: Part 11. An infrared and raman vibrational spectroscopic study of metal(II) halide aniline complexes. *J Mol Structure*. 1982;95:157–168.
38. Ogura T. Complex formation of copper(I) perchlorate with ethylene or carbon monoxide in water and isolation of related complexes. *Inorg Chem*. 1976;15:2301–2303.
39. Yamamoto T, Nakamura Y, Yamamoto A. Study of organo(2,2′-bipyridine)nickel complexes. III. NMR studies on the interaction of diakyl(2,2′-bipyridine)nickel with solvents and olefins. *Bull Chem Soc Japan*. 1976;49:191–197.
40. Bertini I, Luchinat C, Parigi G. *Solution NMR of Paramagnetic Molecules*. New York: Elsevier, 2001.
41. Jung W-S, Ishizaki H, Tomiyasu H. Kinetics and mechanism of ligand exchange in tetrakis(acetylacetonato)zirconium(IV) in organic solvents. *J Chem Soc Dalton Trans*. 1995;1077–1081.
42. Kuroda Y, Aiba H. Contribution of minor species to paramagnetic line broadening of 1H nuclear magnetic resonance spectra in peptide-copper(II) system. *J Am Chem Soc*. 1979;101:6837–6842.
43. Pearson RG, Lanier RD. Rate of rapid ligand exchange reactions by nuclear magnetic resonance line broadening studies. *J Am Chem Soc*. 1964;86:765–771.
44. Cambridge Isotope Laboratories. *NMR Solvent Data Chart*. Available at: http://www.chem.umd.edu/NMR/reference/isotope_solvent.pdf. Accessed on April 20, 2009.
45. National Institute of Advanced Industrial Science and Technology. *Spectral Database for Organic Compounds SDBS*. Available at: http://riodb01.ibase.aist.go.jp/sdbs/cgi-bin/direct_frame_top.cgi. Accessed on April 28, 2009.
46. Durgaprasad G, Sathyanarayana DN, Patel CC. Infrared spectra and normal vibrations of *N,N*-dimethylformamide and *N,N*-dimethylthioformamide. *Bull Chem Soc Jpn*. 1971;44:316–322.
47. Brown WH, Foote CS, Iverson BL. *The unique structure of amide bonds*. In: *Organic Chemistry*, *4th ed*. United States: Thompson Brooks/Cole, 2005:687–688.

Manuscript received Dec. 2, 2009, and revision received Apr. 13, 2010.